General Disclaimer

One or more of the Following Statements may affect this Document

- This document has been reproduced from the best copy furnished by the organizational source. It is being released in the interest of making available as much information as possible.

- This document may contain data, which exceeds the sheet parameters. It was furnished in this condition by the organizational source and is the best copy available.

- This document may contain tone-on-tone or color graphs, charts and/or pictures, which have been reproduced in black and white.

- This document is paginated as submitted by the original source.

- Portions of this document are not fully legible due to the historical nature of some of the material. However, it is the best reproduction available from the original submission.

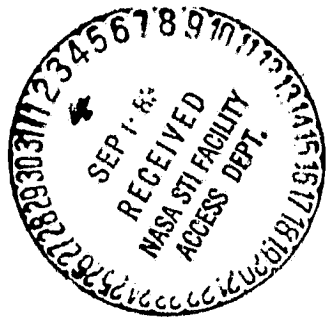

NASA Contractor Report 168213

A Method of Predicting Flow Rates Required to Achieve Anti-Icing Performance with a Porous Leading Edge Ice Protection System

David L. Kohlman and Alan E. Albright

Flight Research Laboratory
University of Kansas Center for Research, Inc.
Lawrence, Kansas 66045

Prepared for

NATIONAL AERONAUTICS AND SPACE ADMINISTRATION
Lewis Research Center
Under Grant NAG 3-71

TABLE OF CONTENTS

	Page
NOMENCLATURE	iii
INTRODUCTION	1
SYSTEM DESCRIPTION	1
PREDICTION METHOD	2
PREDICTED AND ACTUAL FLOW RATES	8
REFERENCES	21

NOMENCLATURE

Symbol	Definition
d	Volume median water droplet diameter
G	Glycol mass fraction in glycol-water solution
LWC	Liquid water content in atmosphere
M_w	Mass rate of water droplet impact per unit area on wing surface
T_a	Ambient freestream temperature
T_f	Freezing temperature of glycol-water solution
T_o	Stagnation temperature
V	True airspeed
V_e	Equivalent airspeed
W_f	Rate of flow of glycol solution per unit area
X	Glycol mass fraction in glycol-water solution pumped through porous leading edge

Greek Symbol	
α	Angle of attack
β	Local catch efficiency

Subscripts	
L	Lower panel
U	Upper panel
max	Maximum

INTRODUCTION

The concept of pumping a glycol-water solution through a porous leading edge skin to achieve ice protection is not new. Operational systems using this concept have been employed on European airplanes for many years. However, no U.S. manufacturers have used liquid anti-ice protection for wing and tail leading edges up to this time. Recently there has been a surge of interest in the U.S. in this concept because of the potential advantages it offers in comparison with pneumatic boots and hot air bleed systems.

Several icing tunnel tests with liquid ice protection systems have been conducted in the NASA Lewis Icing Research Tunnel during the past few years to add to a relatively meager data base. The purpose of this report is to present a proposed method of analytically predicting the minimum fluid flow rate required to provide anti-ice protection with a porous leading edge system on a wing under a given set of flight conditions. Results of the proposed method are compared with the actual results of an icing test of a real wing section in the NASA Lewis Icing Research Tunnel. This work was conducted under NASA Grant NAG 3-71.

SYSTEM DESCRIPTION

A fluid ice protection system consists of a porous leading edge panel attached to the leading edge of a wing and a pump that distributes a glycol-water solution from a reservoir to the leading edge panel through nylon tubing. The fluid flows through the panel onto the surface of the wing, providing either an anti-icing capability by dis-

solving supercooled water droplets and preventing the formation of ice, or a de-icing capability by chemically breaking the bond of established ice. A significant feature of the system is that protection is obtained aft of the panel by the flow of the fluid along the chord to the trailing edge, which often prevents the formation of ice anywhere aft of the active leading edge.

The porous panel material most commonly used consists of two or three layers of stainless steel wire cloth that are rolled, sintered, and finish rolled to proper thickness. Recent development programs have also produced porous panels made of laser-drilled titanium sheet and various composite materials.

A typical cross section of a porous leading edge panel installation is shown in Figure 1. The edges of the active portion of the panel must be placed such that extreme positions of the stagnation point for which icing protection is required are not too close to the edge to prevent fluid from being distributed on both the upper and lower surfaces of the wing.

PREDICTION METHOD

Anti-ice protection is obtained by providing a glycol-water solution on the leading edge of the wing that mixes with the atmospheric water droplets as they impact on the leading edge. To provide anti-ice protection, the resulting solution must have a glycol mass fraction that is high enough to prevent any freezing at the leading edge or on the wing upper and lower surfaces as the fluid flows aft along the wing.

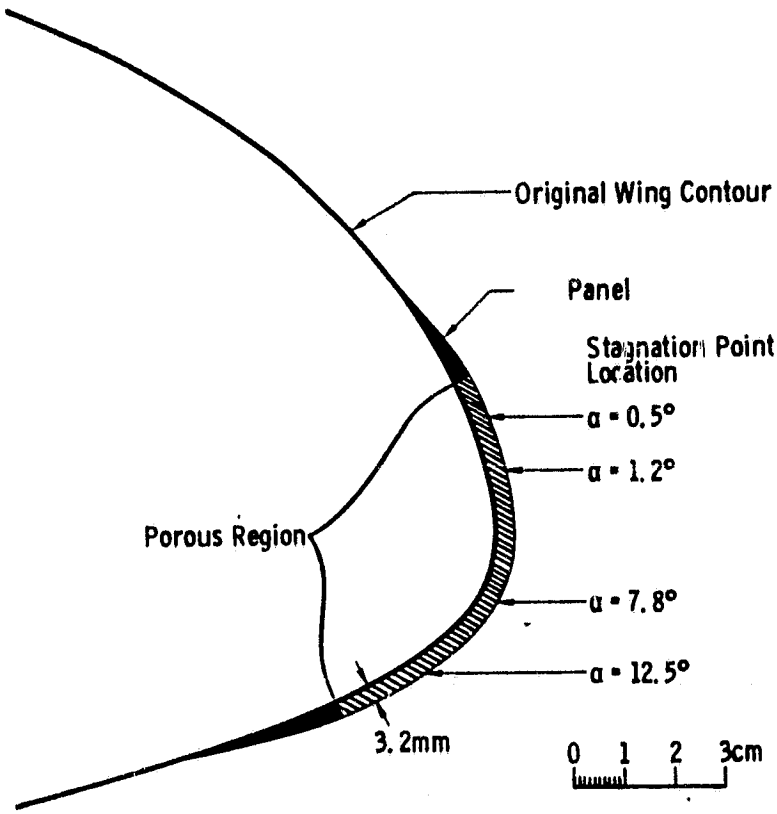

Figure 1: Cross Section of a Porous Panel Installed on a Wing Leading Edge.

The water droplets do not impact as a uniform mass rate on the leading edge. The mass rate per unit area tends to be highest at or near the stagnation point and decreases in a chordwise direction on either side of the stagnation point. The distribution of water mass rate on the leading edge is described by the nondimensional catch efficiency parameter β. The actual local water mass rate of impact per unit area is given as

$$M_w = \beta(LWC)(V). \qquad (1)$$

A typical distribution of β is shown in Figure 2. The trajectories of the water droplets relative to the flow streamlines determine the β distribution. Thus β is a function of the airfoil shape and size, the remote airspeed, the air density, and water droplet diameter. Given β, and the airspeed, the local and total mass rate will be directly proportional to liquid water content.

Until recently, the only methods of predicting β were empirical and semi-empirical. However, the development of improved methods of computational aerodynamics has resulted in several different computer codes that predict β distributions with relatively good accuracy (References 1 and 2).

In contrast to the β distribution, the glycol-water fluid pumped through the porous leading edge is assumed to be distributed at a uniform rate over the surface of the porous skin as shown in Figure 3.

The basic assumption of the proposed prediction method is that the minimum glycol flow rate that will still achieve anti-icing (no ice accumulated on the leading edge), results in a freezing temperature of the glycol-water mixture, at the point of maximum water catch rate, that is equal to the local air temperature. At this point on the wing

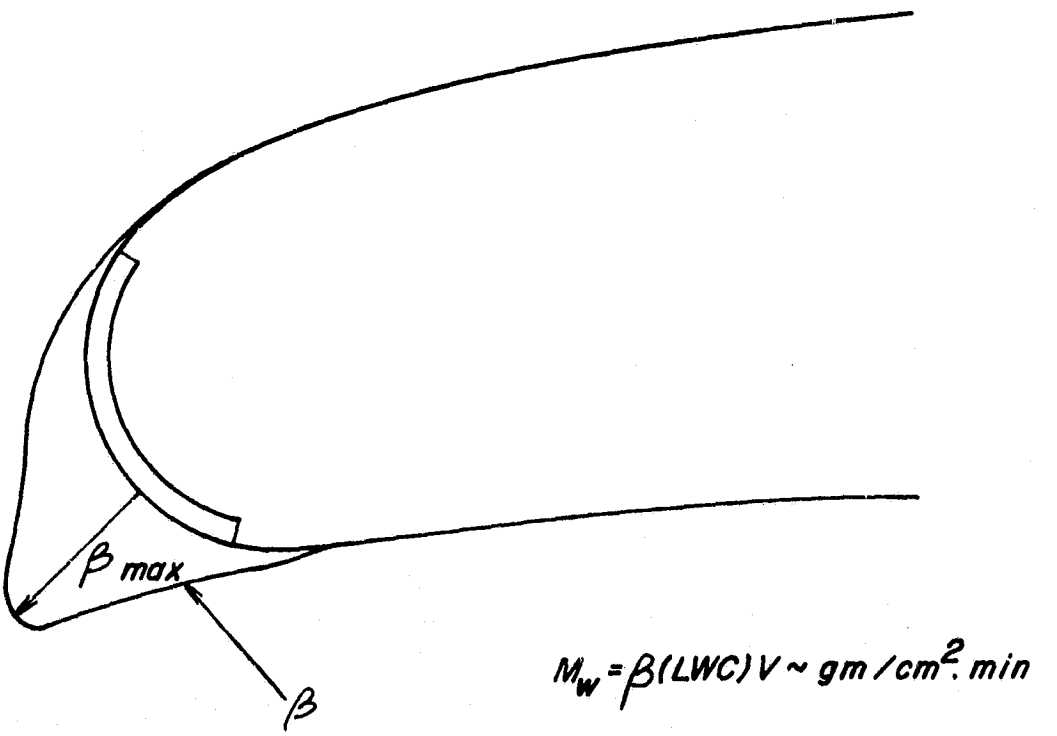

Figure 2: Typical Distribution of Catch Efficiency, β, on a Wing Leading Edge.

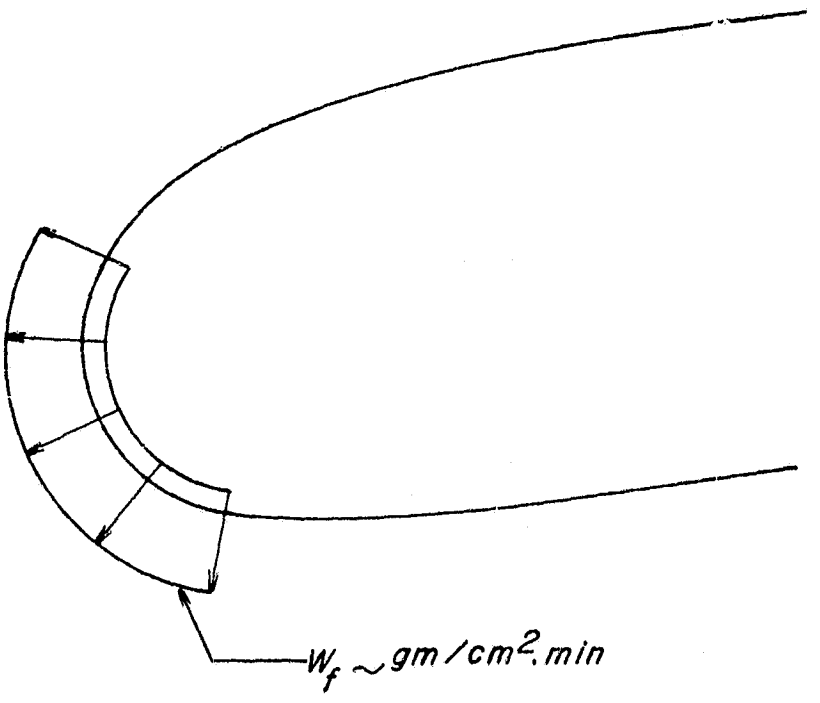

Figure 3: Distribution of Glycol Flow Rate on Porous Leading Edge.

(near or at the stagnation point), the glycol concentration is minimized; and at the anti-ice threshold the mixture will just begin to exhibit the formation of small pieces of ice. As the glycol flow rate is decreased, the extent of ice formation gradually increases until continuous bars are formed spanwise on the leading edge before being swept away every few minutes. This latter mode is called natural deicing.

Obviously, to determine the appropriate glycol rate, the local air temperature must be known. This temperature will be between stagnation temperature and ambient atmospheric temperature. To be conservative, one would choose ambient temperature because it will require a lower freezing temperature and higher flow rate. However, if a constant flow rate is chosen based on the most severe icing conditions anticipated, it is probably sufficient to use stagnation temperature as the local glycol-water freezing temperature. In this case, the system will perform somewhere between an anti-ice mode and natural deice mode during the most severe conditions. Reference 3 shows that the flow rate required for natural deicing is only 25% to 50% of that required for anti-icing. At less severe icing conditions, the system will have a flow rate equal to or greater than that required for anti-icing. As an appropriate compromise, it is suggested that the mean temperature between ambient and stagnation be used.

The method is utilized by following these logical steps.

1. Find β_{max} as a function of
   - airfoil shape
   - airspeed

- air density

- droplet diameter.

Any reasonably accurate computer code, such as those discussed in References 1 and 2, can be used for this step.

2. Calculate the water catch rate M_w by the formula

$$M_w = \beta_{max}(LWC)V. \qquad (1)$$

3. Determine the glycol mass fraction G required to produce a solution with a freezing temperature equal to the average between ambient static temperature and stagnation temperature, using the graph shown in Figure 4. For a glycol mass fraction between 55 and 80%, no clearly defined freezing temperature exists. In practice, this mass fraction, which corresponds with an air temperature below -45°C, would never be required.

4. Calculate the fluid flow required to achieve the glycol mass fraction G, given a water catch rate M_w, by the equation

$$W_f = \frac{GM_w}{X - G} \qquad (2)$$

where X is the initial glycol mass fraction. For most available fluids, X is approximately 0.8.

PREDICTED AND ACTUAL FLOW RATES

To test the validity of this method, it was applied to an airfoil for which anti-ice fluid rates were determined by tests conducted in the NASA Lewis Icing Research Tunnel and reported in Reference 3.

Those tests utilized an actual airplane wing section. The original wing tapered from a NACA 64_2A215 airfoil at the root (WS 0) to a NACA

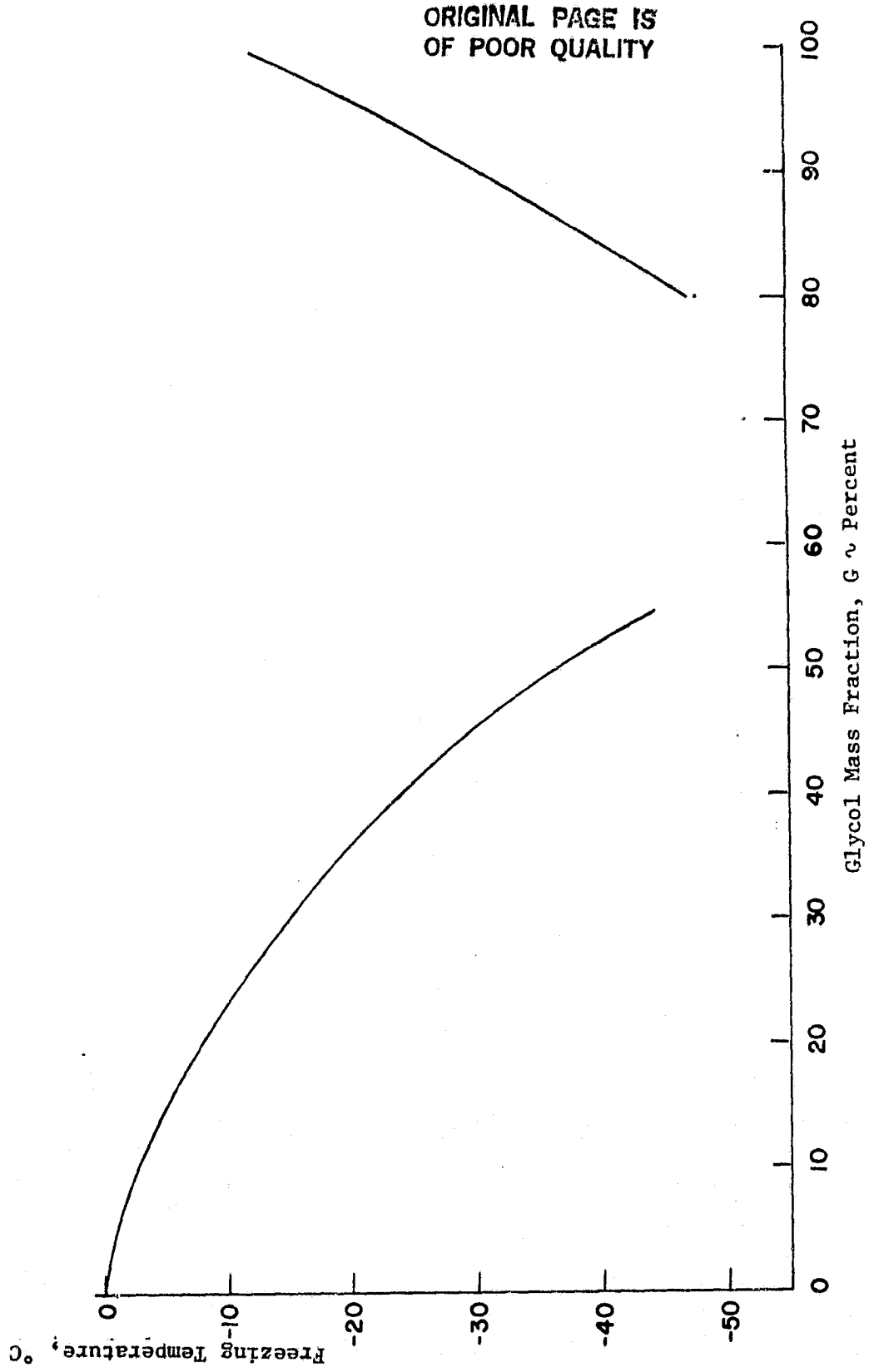

Figure 4: Freezing Temperature of a Monoethylene Glycol-Water Solution.

64_1A412 at the tip (WS 216). The wing incorporated increased thickness on the forward 30% of the upper surface, a modification proposed by R. Hicks of NASA Ames Research Center (Reference 4). The centerline of the tunnel was at WS 58 of the original wing, where the chord is 63.25 in. The predictive method was applied at this station.

The porous panel mounted on the leading edge consisted of three independently controlled sections, with WS 58 in the center of the center section. To obtain the anti-ice flow rates, the upper and lower sections were used simultaneously during each run to establish independent flow rate values while the center section was used to obtain minimum flow rates for natural deicing.

The method of determining the glycol flow rate corresponding with the anti-ice threshold was as follows. At a given flight condition, the flow rate was set to be well above the anti-ice threshold. The flow rate was then reduced in steps, allowing about 30 seconds for the system to stabilize at each point, until small flecks of ice began to appear on the leading edge in the vicinity of the stagnation point. At the anti-ice threshold, the small ice flecks, ranging up to about 3 mm in diameter, would form and then be swept downstream in only a few seconds. A glycol flow rate lower than the threshold value would allow the ice flecks to persist and grow gradually into larger patches before being shed from the wing. Complete test details may be found in Reference 3.

Six test cases were chosen for analysis. Test conditions and flow rate data are presented in Table 1. Also shown are the computed values of β_{max}. The computer code developed at Ohio State University (Reference 2) was utilized.

Table 1: Test Data and Predicted Maximum Catch Rate for an Anti-ice Porous Leading Edge System

Case	V_e kt	LWC gm/m^3	d μm	T_o °F	α deg	W_{f_U} ml/cm^2min	W_{f_L} ml/cm^2min	β_{max}
I	96	1.50	15	25	7.8	.0255	.0193	.208
II	96	2.40	20	25	7.8	.0436	.0340	.314
III	96	1.16	15	5	1.2	.0420	.0330	.219
IV	175	.65	11	25	1.2	.0240	.0250	.259
V	175	.80	15	25	1.2	.0380	.0350	.329
VI	175	1.16	15	25	1.2	.0540	.0430	.329

To check the validity of the proposed method, the freezing temperature of the glycol-water mixture at the stagnation point, given β and the glycol flow rate, was determined by the following method.

The water catch rate M_w was calculated as

$$M_w = \beta_{max}(LWC)V; \tag{1}$$

then

$$G = \frac{XW_f}{W_f + M_w}. \tag{2a}$$

For these tests, X = 0.8. Knowing G, one can determine the freezing temperature of the glycol-water mixture using the data shown in Figure 4.

To determine the sensitivity of the freezing temperature to β_{max}, calculations were made for a range of β_{max} above and below the computed value of β_{max} for each case. Also the sensitivity of freezing temperature to the glycol flow rate was determined by varying W_f above and below the experimentally observed values of W_f at the anti-icing threshold by 20% while holding the value of β_{max} constant.

Results of the calculations are presented in Figure 5 for the six test cases.

Curves are presented for the upper and lower panels. The center panel, where β_{max} was calculated, would be expected to produce a curve between the upper and lower panel. The consistently lower predicted freezing temperature of the upper panel fluid at the stagnation point is apparently caused by the fact that the calculated β_{max} underpredicts the actual value β_{max} for the sharper leading edge of the upper panel of the tapered wing. The reverse is true for the lower panel. There may also be variations in the LWC across the model span.

In every case except for Case 1, the midpoint between the upper and lower panel curves predicts a freezing temperature at the point of β_{max} that lies between the ambient and total air temperature, a result to be expected. This calculated freezing temperature is based on the predicted value of β_{max}, the observed glycol flow rate, the wind tunnel test conditions, and the properties of a glycol-water solution.

The sensitivity of the predicted freezing temperature to errors in the value of β and to variations in the glycol flow rate are illustrated for each case.

It is now useful to compare actual values of W_f with those predicted by the method presented herein. Results are shown in Table 2. Note that the glycol flow rate is converted from volume flow rate to mass flow rate by the specific gravity of the original fluid, which is 1.1.

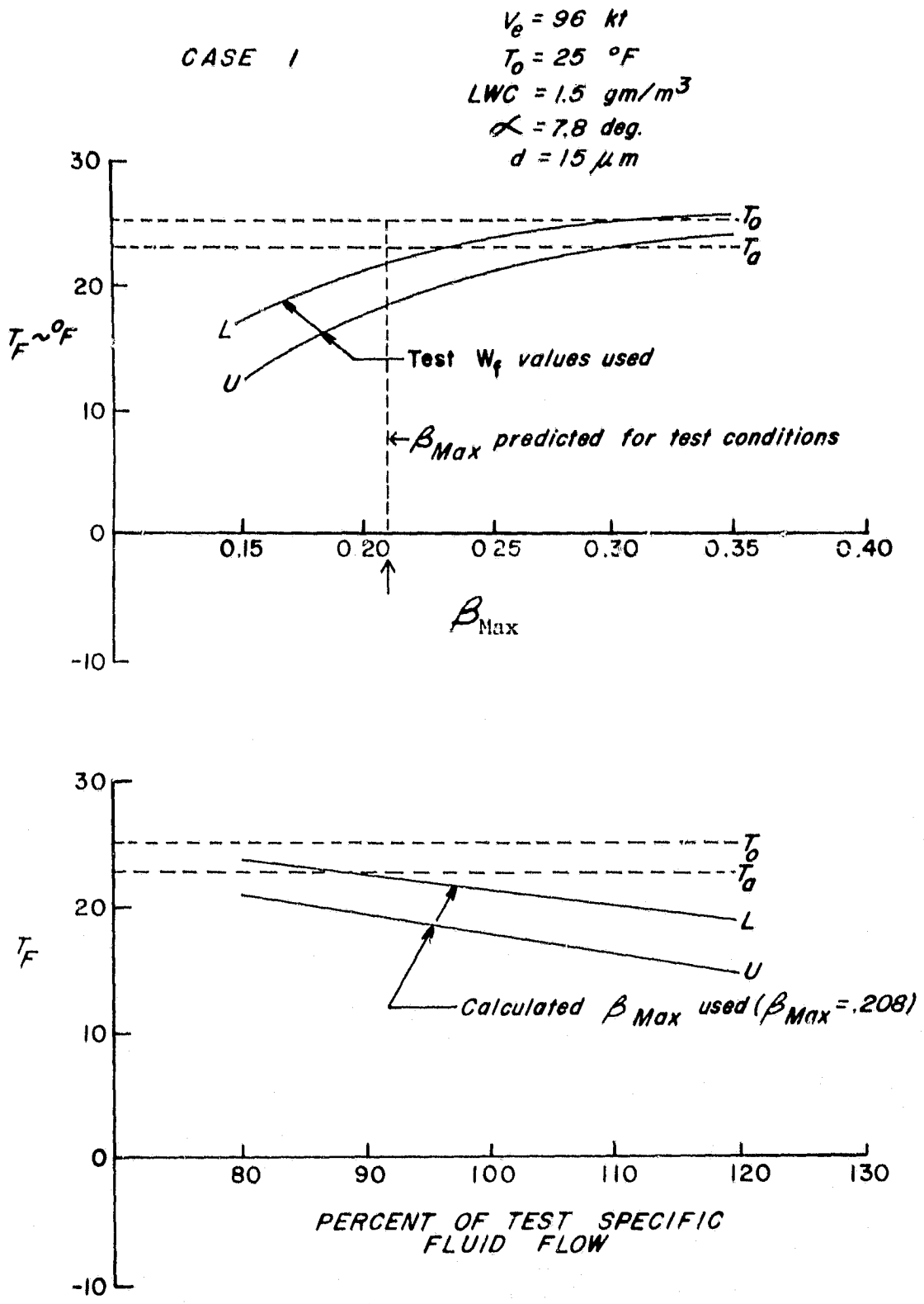

Figure 5: Effect of β_{max} on Local Fluid Freezing Temperature and Effect of Flow Rate on Local Freezing Temperature at Predicted β_{max}. Case I.

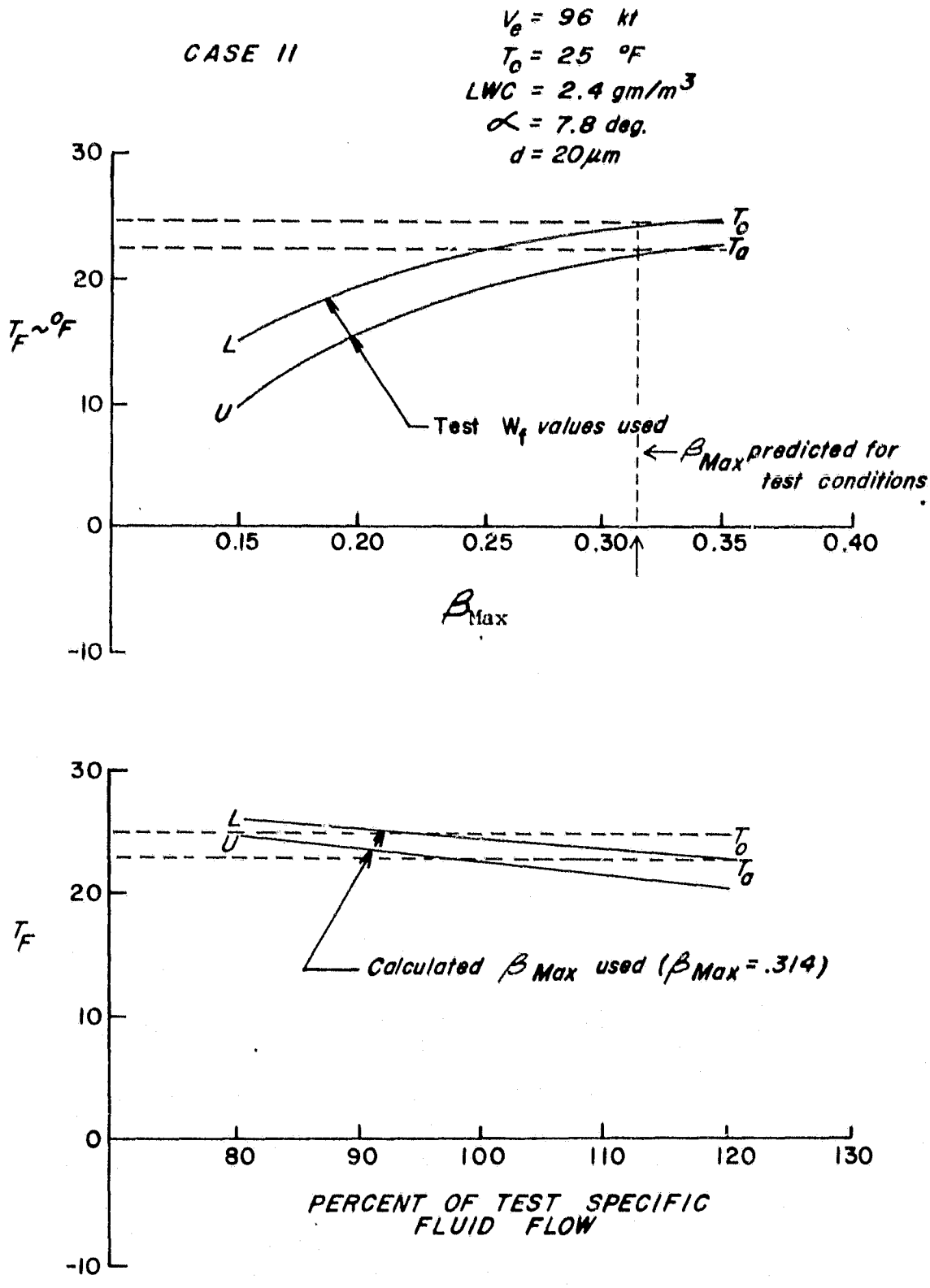

Figure 5: Effect of β_{max} on Local Fluid Freezing Temperature, and Effect of Flow Rate on Local Freezing Temerature at Predicted β_{max}. Case II.

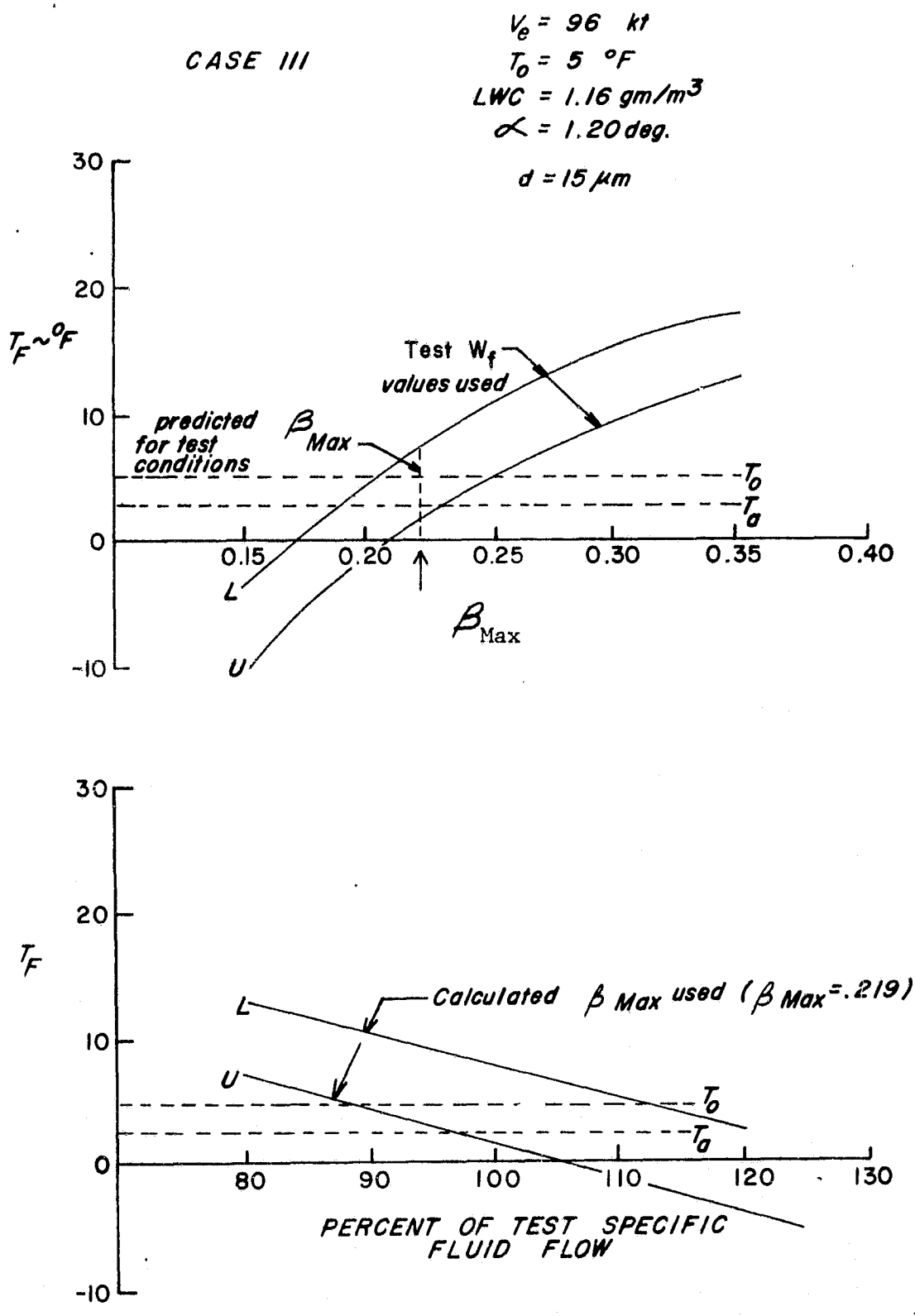

Figure 5: Effect of β_{max} on Local Fluid Freezing Temperature, and Effect of Flow Rate on Local Freezing Temperature at Predicted β_{max}. Case III.

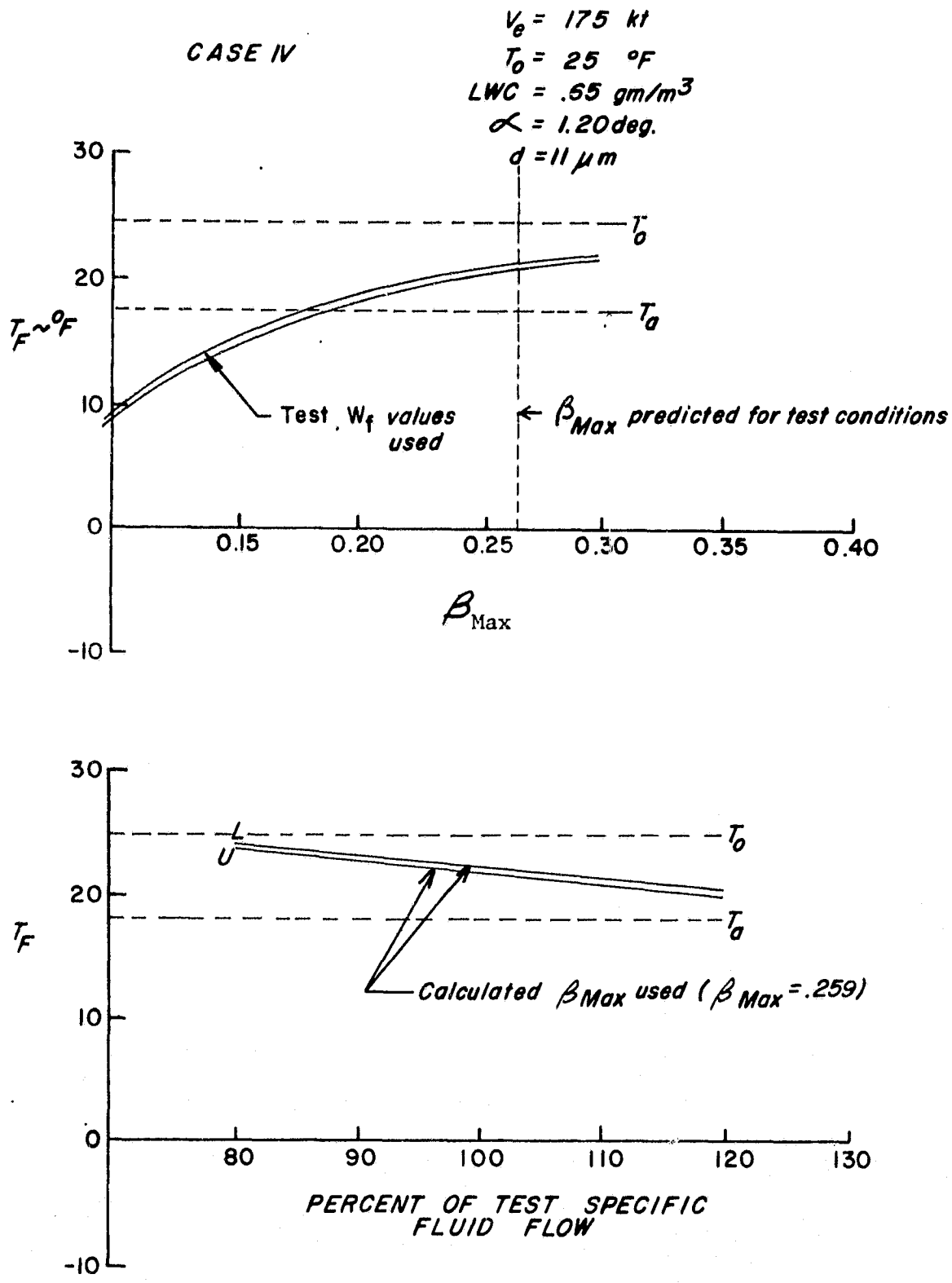

Figure 5: Effect of β_{max} on Local Fluid Freezing Temperature, and Effect of Flow Rate on Local Freezing Temperature at Predicted β_{max}. Case IV.

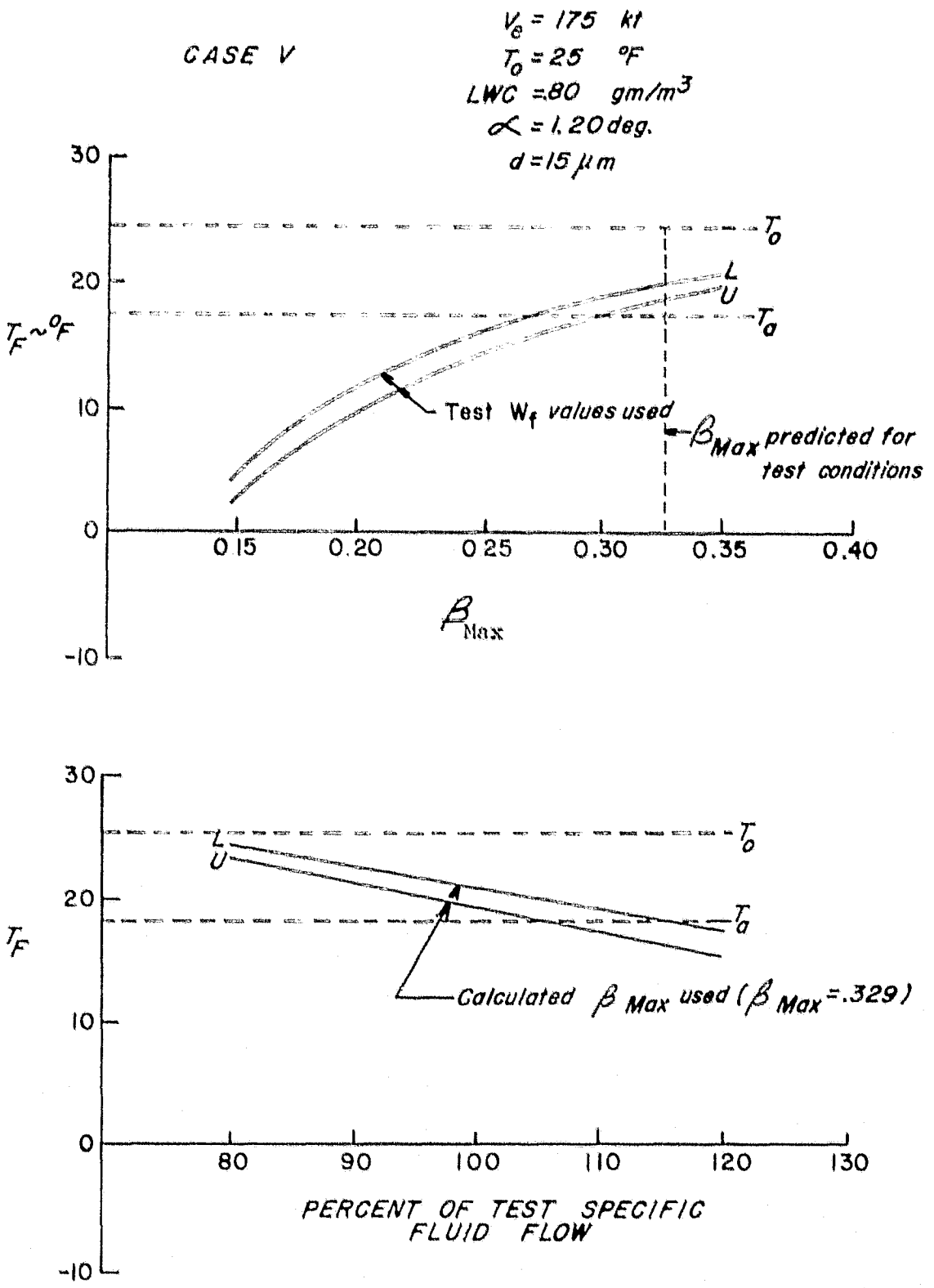

Figure 5: Effect of β_{max} on Local Fluid Freezing Temperature, and Effect of Flow Rate on Local Freezing Temperature at Predicted β_{max}. Case V.

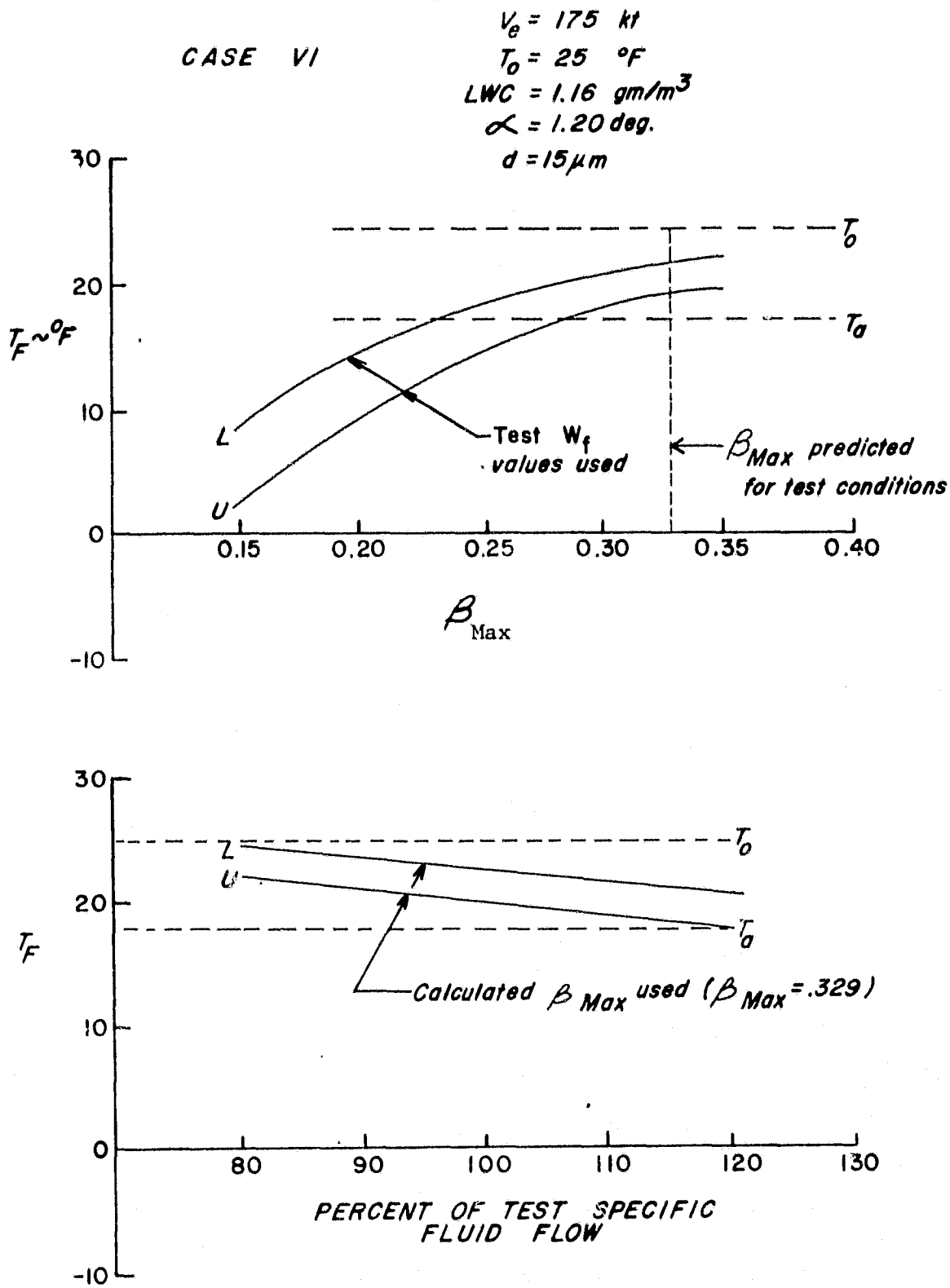

Figure 5: Effect of β_{max} on Local Fluid Freezing Temperature, and Effect of Flow Rate on Local Freezing Temperature at Predicted β_{max}. Case VI.

Table 2: Comparison of Predicted with Actual Test Flow Rates at Anti-icing Threshold

Case	β_{max}	M_w gm/cm^{2}min	$\frac{T_a + T_o}{2}$ deg F	$W_{f_{predicted}}$ gm/cm^{2}min	$\frac{W_{f_U} + W_{f_L}}{2}$ gm/cm^{2}min	Prediction Accuracy %
I	.208	.0837	23.9	.0179	.0246	-27.2
II	.314	.202	23.9	.0432	.0427	+ 1.2
III	.219	.0666	3.9	.0415	.0413	+ .5
IV	.259	.0878	21.5	.0228	.0269	-15.2
V	.329	.137	21.5	.0356	.0401	-11.2
VI	.329	.199	21.5	.0517	.0533	- 3.0

These results show that the method of prediction of anti-ice threshold flow rates presented herein predicts flow rates with an average error of less than 10 percent of the experimentally determined flow rates. This is believed to be excellent, considering the estimated accuracy of the β_{max} prediction and the fact that the anti-icing threshold characteristics tended to persist over a relatively wide range of values of glycol flow rate, making it difficult to obtain fine resolution of the anti-icing threshold. Furthermore, the determination of the anti-icing threshold was somewhat subjective, depending on the judgement of the experimenter.

Therefore, this method appears to provide a reasonably accurate determination of the flow rate required to assure continuous anti-icing performance at a given icing flight condition. For less severe icing, an excess of anti-ice fluid is available at the leading edge. For more severe icing, there will be a gradual transition to a natural

deicing mode which generally provides adequate protection against ice buildup in flight, although this would have to be evaluated for each particular aircraft.

It is recommended that additional testing be done on different airfoils under a variety of test conditions to verify the generality of the method presented in this report.

REFERENCES

1. Frost, W.; Chang, H. P.; Shieh, C. F.; "Two-Dimensional Particle Trajectory Computer Program." NASA CR: to be published.
2. Bragg, Michael B.; "Rime Ice Accretion and Its Effect on Airfoil Performance." NASA CR 165599, March 1982.
3. Kohlman, D. L.; Schweikhard, W. G.; Evanich, P.; "Icing-Tunnel Tests of a Glycol-Exuding, Porous Leading-Edge Ice Protection System." Journal of Aircraft, Vol. 17, No. 8, August 1982, pp. 647-654.
4. Hicks, R. M.; and Schairer, E. T.; "Effects of Upper Surface Modification on the Aerodynamic Characteristics of the NACA 63-215 Airfoil Section." NASA TM 78503, January 1979.